†Research supported in part by the National Science Foundation.

[1]G. Muehllehner, A. S. Poltorak, W. C. Parkinson, and R. H. Bassel, Phys. Rev. 159, 1039 (1967); W. P. Alford and D. G. Burke, Phys. Rev. 185, 1560 (1969); G. R. Satchler, W. C. Parkinson, and D. L. Hendrie, Phys. Rev. 187, 1491 (1969).

[2]Y. E. Kim and J. O. Rasmussen, Phys. Rev. 135, B44 (1964).

[3]J. R. Erskine, Phys. Rev. 135, B110 (1964).

[4]W. P. Alford, J. P. Schiffer, and J. J. Schwartz, Phys. Rev. Letters 21, 156 (1968); W. P. Alford, private communication.

[5]P. Richard, W. G. Weitkamp, W. Wharton, H. Wieman, and P. von Brentano, Phys. Letters 26B, 8 (1967).

[6]C. D. Kavaloski, J. S. Lilley, P. Richard, and N. Stein, Phys. Rev. Letters 16, 807 (1966).

[7]C. F. Moore, L. J. Parish, P. von Brentano, and S. A. A. Zaidi, Phys. Letters 22, 616 (1966).

[8]G. Ballois, J. Saudinos, O. Beer, M. Gendrot, and P. Lopato, Phys. Letters 22, 659 (1966).

[9]G. J. Igo, C. A. Whitten, Jr., Lean-Luc Perreuoud, J. W. Verba, T. J. Woods, J. C. Young, and L. Welch, Phys. Rev. Letters 22, 724 (1969).

[10]A. I. Yavin, R. A. Hoffswell, L. H. Jones, and T. M. Noweir, Phys. Rev. Letters 16, 1049 (1966).

[11]P. S. Miller, Princeton University Technical Report No. PUC-937-339, 1968 (unpublished).

[12]P. S. Miller and G. T. Garvey, to be published.

[13]D. L. Bayer and W. Benenson, Bull. Am. Phys. Soc. 14, 1243 (1969).

[14]E. Kashy, MSUCL Internal Report, 1969 (unpublished).

[15]C. Maples, G. W. Goth, and J. Cerny, University of California Lawrence Radiation Laboratory Report No. UCRL-16964 (unpublished).

[16]J. D. Anderson, C. Wong, and J. W. McClure, Phys. Rev. 138, B165 (1965).

[17]N. Auerbach, J. Hufner, A. K. Kerman, and C. M. Shakin, Phys. Rev. Letters 23, 484 (1969).

[18]W. R. Wharton, P. von Brentano, W. K. Dawson, and P. Richard, Phys. Rev. 176, 1424 (1968).

[19]B. L. Anderson, J. P. Bondorf, and B. S. Madsen, Phys. Letters 22, 651 (1966).

[20]C. J. Batty, B. Bommer, E. Freidman, C. T. Schaler, A. S. Cloagh, J. B. Hunt, and L. E. Williams, Nucl. Phys. A116, 643 (1968).

[21]P. Richard, in Nuclear Isospin, edited by J. D. Anderson, S. D. Bloom, J. Cerny, and W. W. True (Academic Press Inc., New York, 1969), p. 547 and Refs. therein.

[22]G. M. Crawley, P. S. Miller, and D. L. Bayer, Bull. Am. Phys. Soc. 15, 626 (1970).

[23]S. A. A. Zaidi and P. Dyer, Phys. Rev. 185, 1332 (1969).

# Experimental Studies of Neutron-Deficient Gadolinium Isotopes.
## I.    The Electron-Capture Decay of Gd$^{149}$

R. E. Eppley and Wm. C. McHarris

*Department of Chemistry\* and Cyclotron Laboratory,† Department of Physics, Michigan State University, East Lansing, Michigan 48823*

and

W. H. Kelly

*Cyclotron Laboratory,† Department of Physics, Michigan State University, East Lansing, Michigan 48823*

(Received 16 March 1970)

$\gamma$ rays emitted in 9.4-day Gd$^{149}$ have been studied with Ge(Li) and NaI(Tl) detectors. 25 $\gamma$ rays have been attributed to the decay of Gd$^{149}$ with energies and relative intensities of 149.6 (233), 214.5 (0.81), 252.3 (1.1), 260.5 (5.8), 272.0 (15), 298.5 (127), 346.5 (≡100), 405.5 (3.7), 430 (0.33), 459.9 (2.4), 478.7 (0.95), 496.4 (7.2), 516.4 (11), 534.2 (13), 645.2 (5.9), 663.3 (1.1), 666.2 (3.9), 748.2 (35), 788.6 (30), 812.4 (0.55), 863 (0.32), 875.8 (0.90), 933.3 (2.2), 939.1 (9.0), and 947.7 keV (3.7). On the basis of coincidence and anticoincidence experiments, relative intensities, and energy sums, states in Eu$^{149}$ have been placed at 0, 149.6, 459.9, 496.2, 534.2, 666.0, 748.2, 794.8, 812.4, 875.8, 933.3, 939.1, and 1097.3 keV. The Eu$^{149}$ x-ray intensity has also been measured. From our $\gamma$-transition intensities and published conversion-electron intensities, conversion coefficients were obtained for most of the electromagnetic transitions, thus allowing multipolarity assignments to be made for these transitions. These assignments, together with the log$ft$ values, were then used for the placement of limits on the spins of the deduced levels. Our proposed decay scheme is compared with previously published decay schemes and is discussed in terms of current models.

## I.    INTRODUCTION

Neutron-deficient Gd isotopes lie in a region of special interest for the testing of nuclear models. They and their Eu daughters range from nuclei that have large quadrupole moments, suggesting permanently deformed nuclei, through closed-shell nuclei that can be described by an extreme single-

particle shell model. The heavier isotopes ($N \geqslant 90$) are permanently deformed and exhibit well-developed rotational bands and other features that have been described successfully by the Bohr-Mottelson unified model. Spherical nuclei appear as one approaches the closed neutron shell at $N = 82$. It would be of considerable interest to be able to correlate the nuclear levels, especially in the odd-mass nuclei where single-particle states are most easily observed, as one moves from the spheroidal region into the spherical region, and we have embarked on a program to do this, primarily through the study of the radioactive decay of neutron-deficient Gd isotopes. As $Gd^{152}$, $Gd^{154}$ through $Gd^{158}$, and $Gd^{160}$ are stable ($Gd^{152}$ is slightly $\alpha$ active), $Gd^{153}$ is the isotope nearest stability which permits the study of Eu states. And, because the decay schemes of $Gd^{153}$ and $Gd^{151}$ are fairly well characterized,[1,2] the logical place to begin the experimental investigation was with $Gd^{149}$.

9.4-day $Gd^{149}$ was first discovered in 1951 by Hoff, Rasmussen, and Thompson,[3] who produced the isotope by the reactions, $Eu^{151}(p, 3n)Gd^{149}$ and $Sm^{147}(\alpha, 2n)Gd^{149}$. Since that beginning, several papers have been published on its partial decay scheme. Because of the complexity of the $\gamma$-ray spectrum, however, the earlier investigations[3-5] that used NaI(Tl) detectors did not observe a number of the weaker and/or more closely spaced lines, because of the inherently poor resolution of these detectors.

However, even in more recent investigations, in which Ge(Li) detectors[6,7] and conversion-electron detectors[8-11] were employed, discrepancies remain as to many of the $Eu^{149}$ energy levels and also even with respect to which transitions properly follow $Gd^{149}$ decay. In particular, there has been disagreement in the placement of transitions appearing at 993, 1013, and 1082 keV in the $\gamma$-ray spectrum. We undertook the present investigation to try to eliminate some of these uncertainties.

$Gd^{149}$ decays almost exclusively by electron capture, although a small $\alpha$ branch of $4.6 \pm 1.5 \times 10^{-6}$ and an energy of $3.01 \pm 0.02$ MeV has been reported.[12] We have been able to put an upper limit of $10^{-3}(\beta^+/K)$ on the positron branch (cf. Sec. IV). This means that the electromagnetic transitions become the exclusive tool for its study. Very good conversion-electron data already existed, so we made use of these and have concentrated on the photon spectra and coincidence and anticoincidence experiments.

## II. SOURCE PREPARATION

$Gd^{149}$ was prepared by the reaction $Eu^{151}(p, 3n)$-$Gd^{149}$. Both natural europium oxide (47.82% $Eu^{151}$,

52.18% $Eu^{153}$) and separated isotope (96.83% $Eu^{151}$, 3.17% $Eu^{153}$) obtained from the Isotopes Division, Oak Ridge National Laboratory, were used in the proton bombardments. The proton beam was furnished by the Michigan State University sector-focused cyclotron, using a beam energy of 28 MeV with a typical current of 2 $\mu$A. Typically, 100-mg targets were bombarded for periods of 1–2 h.

For the first few hours after the bombardments several short-lived peaks were evident in the spectra. However, after these disappeared, essentially pure $Gd^{149}$ remained. This happy circumstance results because other $(p, xn)$ reactions that should be possible have product nuclei with long half-lives. Activity resulting from the decay of the daughter $Eu^{149}$ ($t_{1/2} = 106$ day) did not show up for several days. However, some spectra (particularly for the anticoincidence runs and for the study of the 993-, 1013-, and 1082-keV peaks) were obtained after chemical separation of Gd from the target material. Two different methods of chemical separation were employed.

The first method was the utilization of Zn-HCl reduction.[13] Owing to a semistable $Eu^{++}$ state, Eu can be separated from the reduction mixture by precipitation with $H_2SO_4$. This technique, carried out two successive times on the target material, yields quite pure (as to the radioactive components) $Gd^{149}$. For $\gamma$-ray analysis this was the only step necessary. When the source must be essentially "mass free," as for an electron source, the $Zn^{++}$ must be removed. This can be accomplished by extraction of the $Zn^{++}$ from the mixture with methyl-isobutyl ketone (hexone).

The second method of separation used was cation exchange.[14,15] The resin beds were composed of Dowex 50 ×8 resin (200–400 mesh) and were 4–5 cm in length and 2 mm in diameter. An isopropyl alcohol bath was used to maintain the column temperature at 83°C during the separation. The eluting agent was 0.4 $M$ $\alpha$-hydroxy-isobutyric acid with the $p$H adjusted to approximately 3.8 by the addition of $NH_3$ solution.

## III. Gd$^{149}$ SPECTRA

### A. Singles Spectra

Two Ge(Li) detectors, both of which were manufactured in this laboratory, were used for all spectra. One was a 7-cm$^3$ five-sided coaxial detector, the other a 3-cm$^3$ planar detector. Both were mounted in dipstick cryostats having aluminum housings 0.16 cm thick. The detectors were used with low-noise room-temperature field-effect transistor preamplifiers, $RC$ linear amplifiers having pole-zero compensation, and 1024- and 4096-channel analyzers.

The Gd$^{149}$ sources were usually counted after having aged several days, but spectra were obtained at times varying from immediately after bombardment to several weeks after bombardment. This technique, together with the chemical separations, enabled us to identify impurity $\gamma$ rays.

The $\gamma$-ray energies were determined by comparison with the standards listed in Table I. The larger peaks were first determined by counting the Gd$^{149}$ sources simultaneously with these standards. The weaker peaks, which would be obscured by the standards, were later determined by using the then well-determined stronger Gd$^{149}$ peaks as internal standards. The centroids of the standard peaks were determined by using a computer program[16] that first subtracts the background by performing a cubic least-squares fit to several channels on each side of the peak. The channels included in the peak are fit to a quadratic curve to determine the centroid, and the centroids of the peaks are fit to a least-squares $n$th degree curve, which becomes the calibration curve. This calibration curve, in turn, is used to determine the energies of the unknown peaks by a similar process.

The relative peak intensities were determined from the peak areas with the use of relative-photopeak-efficiency curves for both Ge(Li) detectors. The curves were obtained by the use of a set of standard $\gamma$-ray sources whose relative intensities have been carefully measured repeatedly with a NaI(Tl) detector.

We have identified 25 $\gamma$ rays as resulting from the $\epsilon$ decay of Gd$^{149}$. Singles spectra are shown in Fig. 1 (separated Eu$^{151}$ target) and Fig. 2 (natural Eu target). A list of the $\gamma$-ray energies and intensities is given in Table II. These energies and intensities are average values from many runs in which various counting geometries, both detectors, and different combinations of associated electronics were used. The listed errors are the over-all experimental errors determined as one half of the range of the values obtained for all the runs included for each average value.

The $K$ x-ray intensity was obtained by a direct comparison with Ce$^{141}$, of which 70% decays to the 145.4-keV state of Pr$^{141}$. The ratio of $K$ x rays to 145.4-keV $\gamma$ rays has been measured[17] to be 0.341 $\pm$ 0.010. The area ratio [$K$ x ray/149.6-keV $\gamma$] for Gd$^{149}$ was measured to be 2.45. When corrected for efficiency by the Ce$^{141}$ ratio, this becomes 2.01. The errors involved should be quite small even through the efficiency curves are changing rapidly in this region, because the energies of the Gd$^{149}$ and Ce$^{141}$ x rays and $\gamma$ rays are so similar.

As can be seen from the singles spectrum resulting from the bombardment of separated Eu$^{151}$ (Fig. 1), peaks are present at 963, 993, and 1013 keV

TABLE I. $\gamma$-ray energy standards.

| Nuclide | $\gamma$-ray energies (keV) | Reference |
|---|---|---|
| Am$^{241}$ | 50.545 $\pm$ 0.031 | a |
| Ce$^{141}$ | 145.43  $\pm$ 0.02 | b |
| Cm$^{243}$ | 209.85  $\pm$ 0.06 | c |
|  | 228.28  $\pm$ 0.08 | c |
|  | 277.64  $\pm$ 0.02 | c |
| Cs$^{137}$ | 661.595 $\pm$ 0.076 | d |
| Mn$^{54}$ | 834.85  $\pm$ 0.10 | e |
| Co$^{60}$ | 1173.226 $\pm$ 0.040 | f |
|  | 1332.483 $\pm$ 0.046 | f |
| Co$^{56}$ | 846.4  $\pm$ 0.5 | g |
|  | 1038.9  $\pm$ 1.0 | g |
|  | 1238.2  $\pm$ 0.5 | g |
|  | 1771.2  $\pm$ 1.0 | g |
|  | $D$2598.5  $\pm$ 0.5 | g |

[a] J. L. Wolfson, Can. J. Phys. 42, 1387 (1964).

[b] J. S. Geiger, R. L. Graham, I. Bergström, and F. Brown, Nucl. Phys. 68, 352 (1965).

[c] R. E. Eppley, unpublished results, 1969.

[d] D. H. White and D. J. Groves, Nucl. Phys. A91, 453 (1967).

[e] W. W. Black and R. L. Heath, Nucl. Phys. A90, 650 (1967).

[f] G. Murray, R. L. Graham, and J. S. Geiger, Nucl. Phys. 63, 353 (1965).

[g] R. L. Auble, Wm. C. McHarris, and W. H. Kelly, Nucl. Phys. A91, 225 (1967).

in addition to those at lower energies. These three "high-energy" peaks were also seen in many of the bombardments using natural Eu, and they have been reported previously[6] as belonging to the decay of Gd$^{149}$. We questioned this because, as can be seen in Fig. 2, a spectrum taken from an older source (in this case using natural Eu target) no longer contains these transitions. An excitation function was run using a natural europium oxide target with proton beams from 10 to 35 MeV at 5-MeV intervals. The characteristic Gd$^{149}$ peaks first appeared in the 20-MeV spectrum as expected ($Q = -16.9$ MeV) and had all but vanished by 35 MeV, thus exhibiting an excitation function with a width typical of a compound-nuclear reaction. Of the three peaks (961, 993, and 1013 keV) only the 961-keV peak was in evidence in any of these runs. However, it first appeared in the 10-MeV spectrum and continued to be present in all of the higher-energy spectra. It was accompanied by peaks at 121 and 841 keV, these three transitions being characteristic of the decay of the 9.3-h isomeric level of Eu$^{152}$. This activity could easily be made by the Eu$^{151}(n, \gamma)$Eu$^{152m}$ reaction. The peaks at 993 and 1013 keV did not appear in any of the excitation-
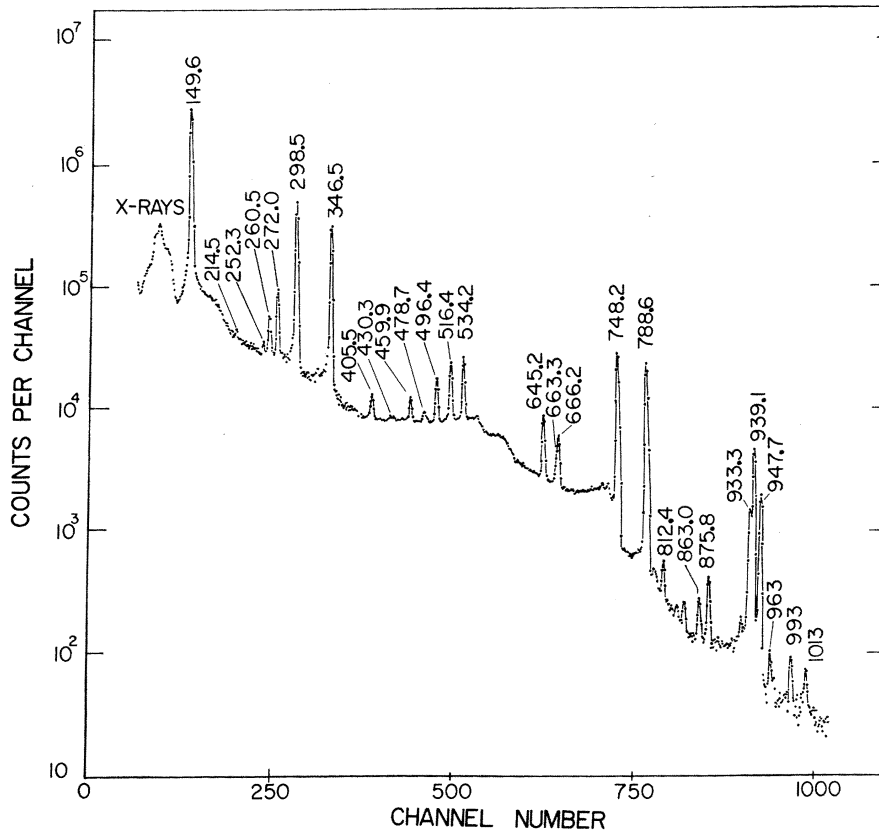
FIG. 1. Gd$^{149}$ singles $\gamma$-ray spectrum from a source prepared with a separated isotope Eu$^{151}$ target taken with a 7-cm$^3$ Ge(Li) detector. Notice the prominence of the 963-, 993-, and 1013-keV peaks. The few peaks which are not labeled on the spectrum are felt not to belong to the decay of Gd$^{149}$.
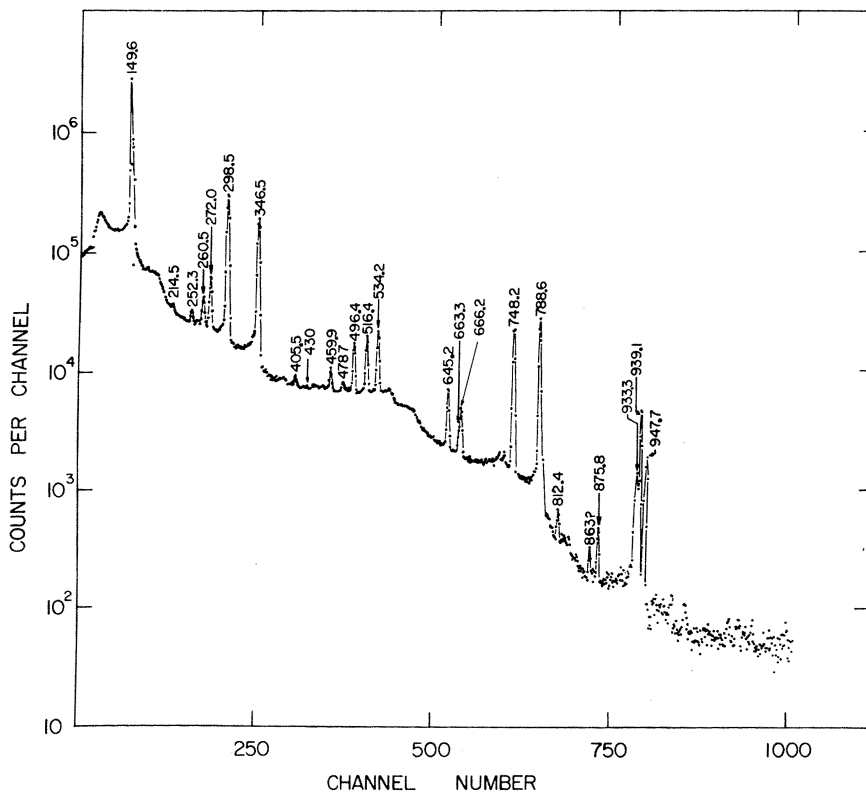


FIG. 2. Gd$^{149}$ singles $\gamma$-ray spectrum from a source prepared with a natural Eu target taken with a 7-cm$^3$ Ge(Li) detector. This source was aged for about a week before counting. The peaks at 963, 993, and 1013 keV are seen to be much less prominent relative to the 947.7-keV peak in this spectrum than they are in Fig. 1.

TABLE II. Energies and relative intensities of $\gamma$ rays from the decay of $Gd^{149}$.

| This work | | Jaklevic, Funk, and Mihelich[a] | | Adam, Toth, and Meyer[b] | |
| --- | --- | --- | --- | --- | --- |
| Energy (keV) | Intensity | Energy (keV) | Intensity | Energy (keV) | Intensity[c] |
| $K$ x rays | 468    ±100 | $K$ x rays | 487    ±35 | ... | ... |
| 149.6±0.2 | 233    ±10 | 150.0±0.5 | 197    ±20 | 149.8 | 258.9    ±20.0 |
| ... | ... | ... | ... | 184.8 | 0.23  ±  0.12 |
| 214.5±0.6 | 0.81±  0.10 | 216.0±0.5 | 1.6±  0.8 | 216 | 0.91  ±  0.40 |
| ... | ... | ... | ... | 230.4 | 0.65  ±  0.31 |
| ... | ... | ... | ... | 235.1 | 0.14  ±  0.07 |
| 252.3±0.7 | 1.08±  0.25 | ... | ... | 252.5 | 0.54  ±  0.15 |
| 260.5±0.3 | 5.80±  0.4 | 262.0±0.5 | 7.0±  0.7 | 260.9 | 4.70  ±  0.80 |
| ... | ... | ... | ... | 264.6 | |
| ... | ... | ... | ... | 267.8 | 0.061±  0.015 |
| ... | ... | ... | ... | 268.6 | |
| 272.0±0.2 | 14.6  ±  0.6 | 272.0±0.5 | 16.1±2 | 272.6 | 11.6   ±  1.0 |
| 298.5±0.2 | 126    ±10 | 298.5±0.5 | 106    ±10 | 298.7 | 114.8   ±  4.9 |
| 346.5±0.3 | ≡100 | 347.0±0.5 | 100    ±10 | 346.8 | 100.0   ±  4.9 |
| 405.5±0.7 | 3.7  ±  1.5 | ... | ... | 404.0 | 0.70  ±  0.30 |
| 430   ±1[d] | 0.33±  0.05 | ... | ... | ... | ... |
| 459.9±0.3 | 2.4  ±  0.2 | 461   ±1 | 2.3±  0.3 | 460.3 | 1.81  ±  0.30 |
| 478.7±0.3 | 0.95±  0.10 | 480   ±1 | 0.4±  0.1 | 478.3 | 1.80  ±  0.51 |
| 496.4±0.3 | 7.2  ±  0.4 | 497.0±0.5 | 7.2±  0.7 | 496.6 | 6.61  ±  1.00 |
| 516.4±0.3 | 11.1  ±  1.5 | 517.0±0.5 | 10.7±1 | 516.8 | 10.30  ±  1.00 |
| 534.2±0.3 | 13.2  ±  0.6 | 534.0±0.5 | 12.5±  1.3 | 534.4 | 13.50  ±  1.00 |
| 645.2±0.3 | 5.9  ±  0.5 | 646.5±0.5 | 7.0±  0.7 | 645.2 | 6.20  ±  0.59 |
| 663.3±0.7 | 1.1  ±  0.2 | ... | ... | 663.4 | 4.51  ±  0.49 |
| 666.2±0.7 | 3.9  ±  0.6 | 666.5±0.5 | 6.0±  0.6 | 666.6 | |
| 748.2±0.3 | 34.6  ±  4.0 | 749.5±0.5 | 37.0±4 | 749.1 | 34.1   ±  4.0 |
| 788.6±0.3 | 29.6  ±  3.0 | 790.5±0.5 | 34.8±4 | 789.3 | 31.2   ±  4.0 |
| 812.4±0.5 | 0.55±  0.31 | 813   ±1 | 0.7±1 | 813.0 | 0.642±  0.149 |
| 863   ±1  ? | 0.32±  0.10 | 865   ±1 | 0.3±  0.05 | ... | ... |
| 875.8±0.4 | 0.90±  0.11 | 878   ±1 | 0.7±  0.1 | 876.2 | 0.980±  0.201 |
| 933.3±0.5 | 2.2  ±  0.5 | 934   ±1 | 2.8±  0.3 | 934 | 2.41  ±  0.30 |
| 939.1±0.4 | 9.0  ±  1.4 | 939.0±0.5 | 12.1±2 | 939.0 | 11.2   ±  2.0 |
| 947.7±0.5 | 3.7  ±  0.6 | 949.0±0.5 | 4.8±  0.5 | 948.0 | 3.70  ±  0.70 |
| ... | ... | 993   ±1 | 1.5±  0.2 | ... | ... |
| ... | ... | 1013   ±1 | 1.3±  0.1 | ... | ... |
| ... | ... | 1082   ±1 | 0.8±  0.1 | ... | ... |

[a]See Ref. 6.

[b]See Ref. 7.

[c]These intensities were obtained by normalizing the intensity (891±44) for the 346.5-keV $\gamma$ as given in Ref. 7 to 100, always retaining the original number of significant figures.

[d]This transition was not seen in the singles spectra but only in the 600-keV region gated spectrum (Fig. 8).

function spectra; however, the statistics were such that very weak peaks at these energies would not be observed. When observed in other singles spectra these two peaks do appear to decay with a half-life similar to, but less than, that of $Gd^{149}$, although no specific half-life determination has been made. It should be noted that, when present, these peaks do remain with the Gd fraction after separation in an ion-exchange process.

### B.  Prompt Coincidence Spectra

Both prompt and delayed spectra were obtained by a variety of methods. The 7-cm³ Ge(Li) detec-

tor was normally used for recording spectra, with a 3×3-in. NaI(Tl) detector setting the gates. For some of the spectra, however, the Ge(Li) detector was placed at one end inside the tunnel of an 8×8-in. NaI(Tl) split annulus.[18] The source was placed on top of the Ge(Li) detector inside the annulus. For an anticoincidence spectrum a 3×3-in. NaI(Tl) detector was placed at the other end of the annulus tunnel in order to subtend a greater solid angle from the source, thereby further reducing the Compton background, in particular the Compton edges resulting from backscattering from the Ge(Li) detector. For all of the coincidence ex-

periments a standard fast-slow coincidence cir-
cuit was used and the lower discriminators of the
single-channel analyzers were adjusted to accept
only pulses with energies greater than those of the
$K$ x rays. For the coincidence runs the resolving
time ($2\tau$) of the fast coincidence unit was $\approx 100$
nsec, while for the anticoincidence run it was
$\approx 200$ nsec.

The anticoincidence and integral- or "any-" co-
incidence spectra are shown in Figs. 3 and 4.
These spectra complement each other in helping
to elucidate the decay scheme. The enhancement
of a peak in the anticoincidence spectrum implies
a ground-state transition either from a level fed
primarily by direct $\epsilon$ decay or from a level with a
half-life long compared with the resolving time;
examples are the 748.2- and 496.4-keV $\gamma$'s. In the
integral-coincidence spectrum such transitions
should be either absent or reduced in intensity.
The integral-coincidence spectrum also confirms
much of the information gained from the individual-
ly gated spectra below. The relative intensities
of peaks in the coincidence runs are given in Ta-
ble III, and a summary of our inferences from
them is given in Table IV.

Other useful coincidence spectra were obtained
by gating on the 149.6-, 346.5-, and 534.2-keV
peaks and on the 600- and 900-keV regions. These
are shown in order in Figs. 5–9. Tables III and IV
again summarize the relevant information from
these spectra, but we defer any detailed discussion
until Sec. V, where points essential to our con-
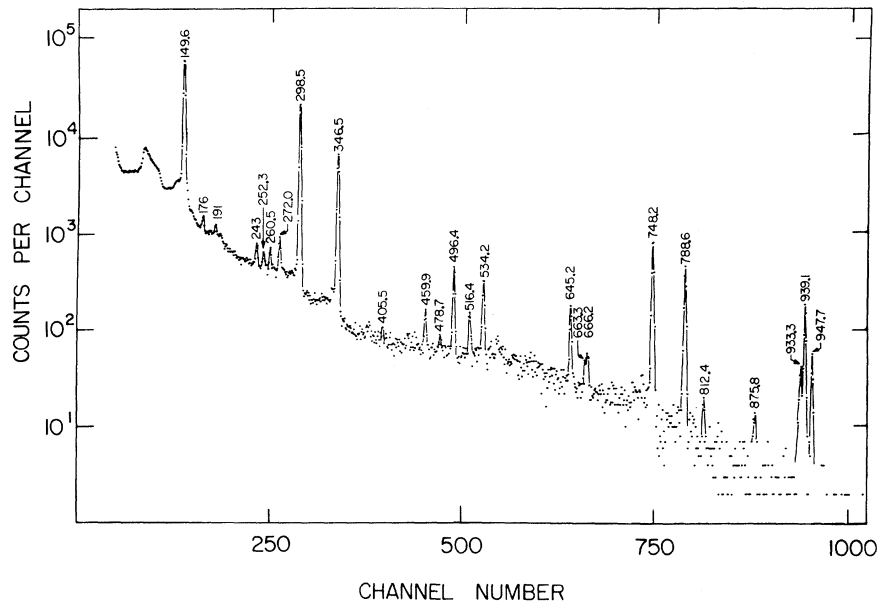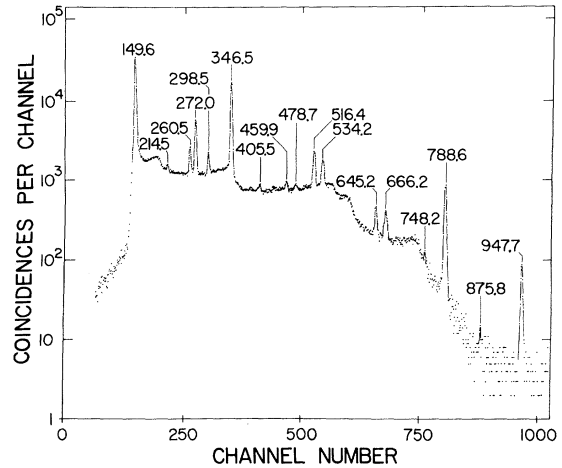struction of the decay scheme will be covered.



FIG. 4. Integral-coincidence spectrum of $Gd^{149}$ taken
with the $7$-$cm^3$ Ge(Li) detector using the $8 \times 8$-in. split-
ring annulus for the gating signals. The fast-coincidence
resolving time was $\approx 100$ nsec.

### C. Delayed Coincidence Studies

Many nuclei in this region have an $h_{11/2}$ isomeric
state, and $Eu^{149}$ is no exception. The 496.4-keV
state was first suggested to be isomeric by Shirley,
Smith, and Rasmussen,[4] who assigned the 346.5-
keV transition as $M2$ on the basis of its conversion
ratios. The half-life of the state was later mea-
sured by Berlovich et al.,[19] to be $2.48 \pm 0.05 \times 10^{-6}$
sec. In several previous studies[5, 6] delayed-coin-
cidence experiments were performed to determine
the feeding of the 346.5-keV state from above, but



FIG. 3. Anticoincidence spectrum of $Gd^{149}$ recorded by the $7$-$cm^3$ Ge(Li) detector when placed inside the tunnel of an
$8 \times 8$-in. NaI(Tl) split annulus, with a $3 \times 3$-in. NaI(Tl) detector at the other end of the tunnel.

TABLE III. Intensities of Gd[149] γ rays in coincidence experiments.

| $E_\gamma$ (keV) | Singles | Anticoincidence | Relative intensity Integral coincidence | 149.6-keV gate | 346.5-keV gate[a] | 534.5-keV gate | 600-keV gate | 900-keV gate |
|---|---|---|---|---|---|---|---|---|
| 149.6±0.2 | 233 ±10 | ··· | 48.4 | ··· | ≡233 | 1.10 | 5.02 | Ref. b |
| 214.5±0.6 | 0.81±0.10 | 1.37 | 0.78 | ··· | ··· | 0.68 | ··· | ··· |
| 252.3±0.7 | 1.08±0.25 | 1.30 | ··· | ··· | ··· | ··· | ··· | ··· |
| 260.5±0.3 | 5.80±0.40 | 1.43 | 5.03 | 2.88 | 6.03 | ≡5.80 | 0.79 | ··· |
| 272.0±0.2 | 14.6 ±0.6 | 2.78 | 18.1 | 33.3 | 14.5 | 6.21 | ≡14.6 | ··· |
| 298.5±0.2 | 126.7 ±10 | 109 | 4.71 | 15.7 | 25.9 | 0.43 | ··· | ··· |
| 346.5±0.3 | ≡100 | 63.7 | ≡100 | 272 | 4.93 | 0.21 | ··· | ··· |
| 405.5±0.7 | 3.7 ±1.5 | ··· | 1.67 | ··· | ··· | 0.87 | 0.12 | ··· |
| 430 ±1 | ··· | ··· | ··· | ··· | ··· | ··· | 0.33 | ··· |
| 459.9±0.3 | 2.4 ±0.2 | 1.41 | 2.80 | ··· | ··· | 0.38 | 0.11 | ··· |
| 478.7±0.3 | 0.95±0.10 | ··· | 1.63 | ··· | ··· | ··· | 0.089 | ··· |
| 496.4±0.3 | 7.2 ±0.4 | ≡7.2 | ··· | ··· | ··· | ··· | ··· | ··· |
| 516.4±0.3 | 11.1 ±1.5 | 1.89 | 23.0 | ≡11.1 | 14.1 | 0.054 | 0.19 | ··· |
| 534.2±0.3 | 13.2 ±0.6 | 6.53 | 14.9 | 2.36 | 5.82 | 0.062 | 0.13 | ··· |
| 645.2±0.3 | 5.9 ±0.5 | 3.83 | 6.1 | 6.22 | ··· | ··· | ··· | ··· |
| 663.3±0.7 | 1.1 ±0.2 ⎱ | 1.81 | 6.34 | 1.11 | ··· | ··· | ··· | ··· |
| 666.2±0.7 | 3.9 ±0.6 ⎰ | | | | | | | |
| 748.2±0.3 | 34.6 ±4.0 | 31.1 | 0.35 | ··· | ··· | 0.048 | ··· | ··· |
| 788.6±0.3 | 29.6 ±3.0 | 18.7 | 28.1 | 16.3 | ··· | ··· | ··· | ··· |
| 812.4±0.5 | 0.55±0.13 | 0.46 | ··· | ··· | ··· | ··· | ··· | ··· |
| 863.1±1.0 | 0.32±0.10 | ··· | ··· | ··· | ··· | ··· | ··· | ··· |
| 875.8±0.4 | 0.90±0.11 | ··· | ··· | ··· | ··· | ··· | ··· | ··· |
| 933.3±0.4 | 2.2 ±0.5 | 2.55 | ··· | ··· | ··· | ··· | ··· | ··· |
| 939.1±0.6 | 9.0 ±1.4 | 9.90 | ··· | ··· | ··· | ··· | ··· | ··· |
| 947.7±0.5 | 3.7 ±0.6 | 2.41 | ··· | ··· | ··· | ··· ○ | ··· | ··· |

[a]Nothing appears to be in prompt coincidence with the 346.5-keV γ except the 149.6-keV γ, and its intensity should be diminished in this spectrum because it is fed by many other γ rays in addition to the 346.5-keV γ. Thus, all the intensities in this column should be regarded as upper limits originating from chance or instrumental effects.

[b]Only peak in spectrum.

TABLE IV. Summary of coincidence data.

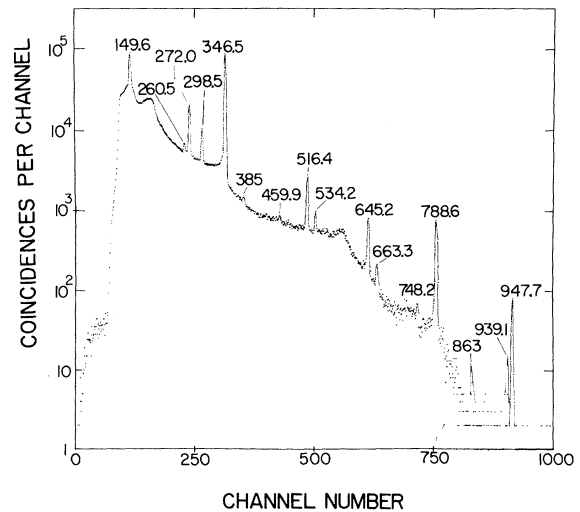| Gate energy (keV) | Peaks in coincidence (keV) | Figure No. |
|---|---|---|
| Integral gate | 149.6, 214.5, 260.5, 272.0, 346.5, 405.5, 459.9, 478.7, 516.4, 534.2, 645.2, 663.3, 666.2, 788.6, 947.7 | 4 |
| 149.6 | 272.0, 346.5, 516.4, 645.2, 663.3, 788.6, 947.7 | 5 |
| 346.5 | 149.6 | 6 |
| 534.2 | 214.5, 260.5, 405.5 | 7 |
| 600 region | 149.6, 272.0, 430.3 | 8 |
| 900 region | 149.6 | 9 |
| 149.6 delayed coincidence | 252.3, 298.5 | 10 |



FIG. 5. Spectrum of γ rays from Gd[149] decay observed in coincidence with the 149.6-keV transition. The spectrum was taken with the 7-cm³ Ge(Li) detector using a 3×3-in. NaI(Tl) detector to provide the gating signals.
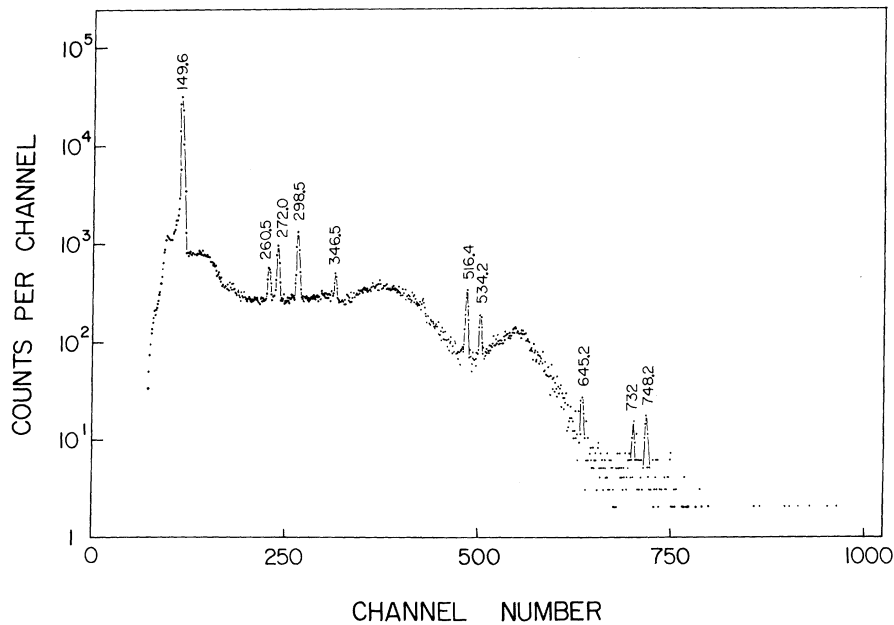
FIG. 6. Gd$^{149}$ coincidence spectrum taken with a prompt gate on the 346.5-keV transitions. Only the 149.6-keV transition is in coincidence with the 346.5-keV transition. The remainder of the peaks actually arise from chance.

we obtain somewhat different results from these.

We used a 3×3-in. NaI(Tl) detector to gate on the 346.5-keV $\gamma$ and on the 149.6-keV $\gamma$ that is in coincidence with it (cf. the decay scheme in Fig. 13 below). The 7-cm$^3$ Ge(Li) detector signal was delayed relative to these gates by inserting passive delays ranging from 0.25 to 0.50 $\mu$sec, depending on the particular run. The fast resolving time $(2\tau)$ again was set at $\approx$100 nsec. The spectrum resulting from the 149.6-keV delayed gate is shown in

Fig. 10, and the intensities of peaks in this spectrum are compared with their intensities in the corresponding prompt spectrum in Table V. A summary of the conclusions is also included in Table IV. The spectrum resulting from the 346.5-keV gate produced essentially the same results, so it is not shown.

In all the delayed spectra the 298.5-keV $\gamma$ was enhanced, indicating that it does indeed feed the 496.4-keV level. There was also some evidence
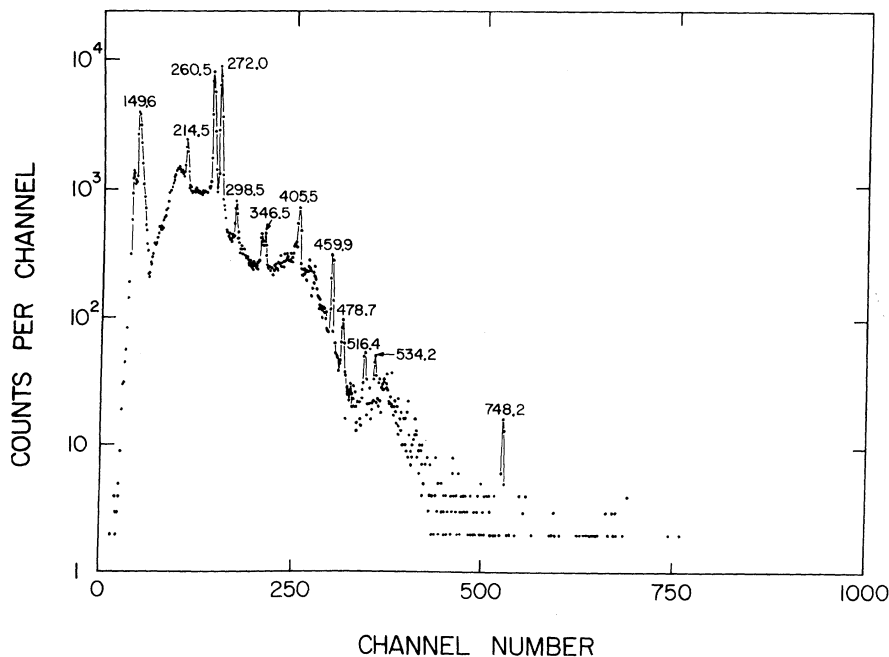


FIG. 7. Coincidence spectrum of Gd$^{149}$ with the gate on the 534.2-keV transitions. The 7-cm$^3$ Ge(Li) detector was used for the spectrum, with the 8×8-in. split-ring annulus being used for the gating signals.

FIG. 8. Gd$^{149}$ coincidence spectrum with the gate set on the 600-keV region. The 7-cm$^3$ detector was again used for the spectrum, with the 8×8-in. annulus used to provide the gating signals. This is the only spectrum in which the peak at 430 keV is enhanced.
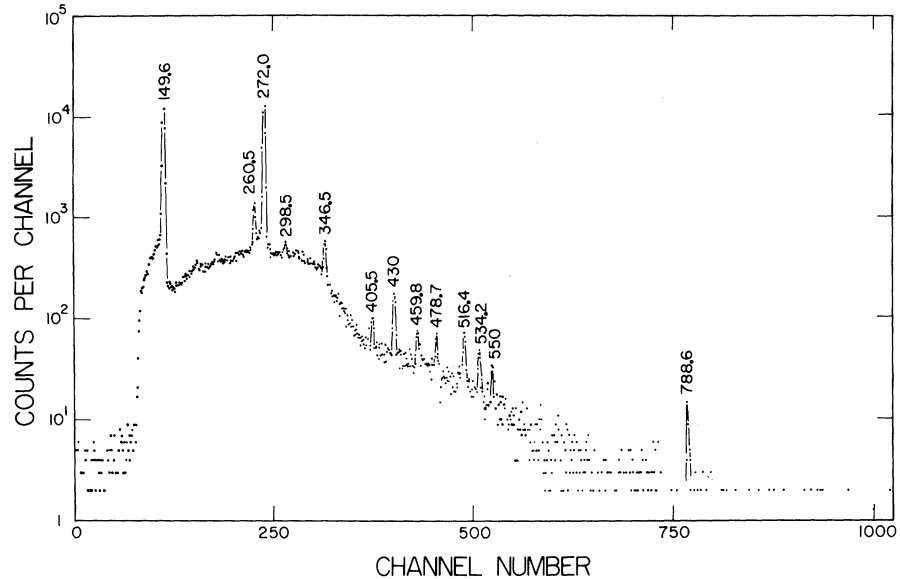
for enhancement of the 252.3-keV $\gamma$. However, the 459.9-keV $\gamma$, which had previously been reported[5,6] as feeding the 496.4-keV level, is completely missing from Fig. 10. This, and other evidence which will be discussed in Sec. V, leads us to the conclusion that the 459.9-keV $\gamma$ does not proceed to the 496.4-keV level but instead depopulates a newly proposed 459.9-keV level.

### D. Internal-Conversion Coefficients

For the determination of internal-conversion coefficients we used the electron intensities reported by Harmatz and Handley,[11] who reported extensive values for $K$ electrons along with some values for $L_I$ and $M_I$ electrons. These values were obtained with flat-field permanent-magnet spectrographs using photographic plates and have reported uncertainties of $\approx 15\%$ for the most prominent lines. For
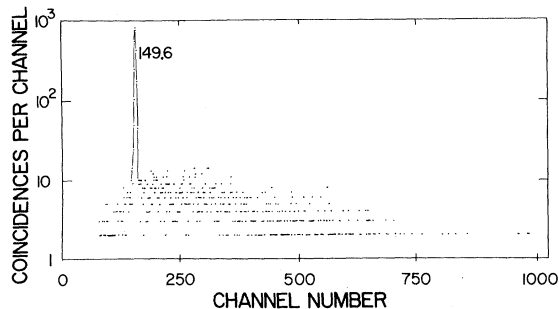


FIG. 9. Gd$^{149}$ coincidence spectrum with the gate set on the 900-keV region. This spectrum, used in conjunction with the 149.6-keV gated spectrum, shows that, of the peaks in the 900-keV region, only the peak at 947.7 keV is in coincidence, it being in coincidence with the 149.6-keV level.
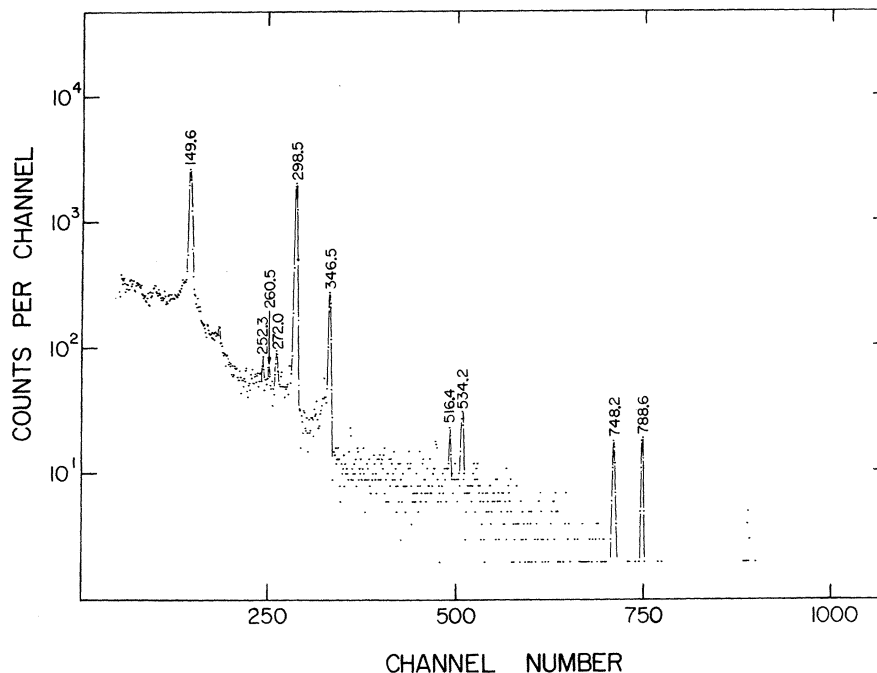
purposes of normalization we assumed the 346.5-keV transition to be pure $M2$ and used the theoretical value of $\alpha_K$ from Hager and Seltzer.[20]

Multipolarities or possible multipolarities were assigned for all transitions where $K$-electron intensities were available. We compared the experimental $\alpha_K$'s with the theoretical $\alpha_K$'s of Hager and Seltzer.[20] Where necessary, (logarithmic) quadratic interpolation was made between the tabular theoretical values. As our lowest energy was 149.6 keV, this method yielded satisfactory results. These theoretical values were used to construct the smooth curves in Fig. 11, upon which we have superimposed the experimental points

TABLE V. Intensities of Gd$^{149}$ $\gamma$ rays in delayed and prompt coincidence.

| $E_\gamma$ (keV) | Relative intensity (normalized to singles intensity) | |
| --- | --- | --- |
| | 149.6-keV delayed | 149.6-keV prompt |
| 149.6 ± 0.2 | 4.78 | ... |
| 252.3 ± 0.7 | 0.85 | ... |
| 260.5 ± 0.3 | 0.86 | 2.88 |
| 272.0 ± 0.2 | 2.08 | 33.3 |
| 298.5 ± 0.2 | ≡126 | 15.7 |
| 346.5 ± 0.3 | 18.2 | 272 |
| 496.4 ± 0.3 | 1.17 | ... |
| 516.4 ± 0.3 | 1.51 | ≡11.1 |
| 534.2 ± 0.3 | 2.73 | 2.36 |
| 645.2 ± 0.3 | ... | 6.22 |
| 663.3 ± 0.7⎱ | ... | 1.11 |
| 666.2 ± 0.7⎰ | | |
| 748.2 ± 0.3 | 5.37 | ... |
| 788.6 ± 0.3 | 5.68 | 16.3 |

FIG. 10. Gd$^{149}$ delayed-coincidence spectrum. The spectrum signal was delayed relative to the gate by adding a 0.5-
$\mu$sec passive delay to the Ge(Li) detector side before it entered the fast-coincidence unit $(2\tau \approx 100$ nsec). In this manner,
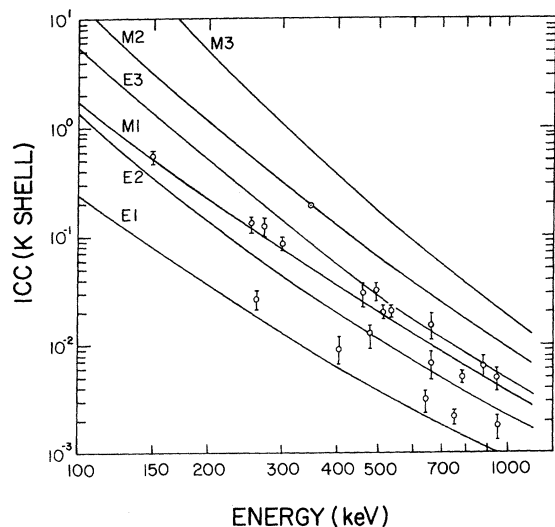the resulting spectrum shows only those transitions feeding the 496.4-keV isomeric level.



FIG. 11. Experimental and theoretical conversion co-
efficients for the transitions in Eu$^{149}$ following the decay
of Gd$^{149}$. These values are also listed in Table VI. The
smooth curves were drawn by using values interpolated
from the tables of Hager and Seltzer (Ref. 20). The er-
ror bars placed on the experimental values are only
crude estimates, since no precise error values were
available for the conversion-electron intensities.

along with their estimated errors (ranging between
15 and 30%).

Some of the multipolarity assignments were cor-
roborated by $K/L_{\rm I}$ or $K/M_{\rm I}$ ratios, although these
are less sensitive indicators than the $K$-conversion
coefficients. The interested reader is referred to
Harmatz and Handley[11] for their $L_{\rm I}$ and $M_{\rm I}$ inten-
sity values.

## IV. ELECTRON-CAPTURE ENERGY

Because there is no measurable $\beta^+$ emission
from the decay of Gd$^{149}$, a direct measurement of
its decay energy is not possible. Various esti-
mates of $Q_\epsilon$ range all the way from 1.220[21] to 2.275
MeV.[22] As an alternative to an arbitrary adoption
of one of the several published values, we made a
graphical estimate of $Q_\epsilon$, using a method similar
to that suggested by Way and Wood[23] and previous-
ly used by Grover.[24]

A plot (Fig. 12) was made of all experimentally
known decay energies versus $Z$ for pairs of nuclei
having the same neutron numbers as the pair for
which the decay energy is to be determined. Both
electron-capture and $\beta^-$ decay pairs were plotted,
and for our particular graph, as $Q_\epsilon$ is chosen to be
positive and $Q_{\beta^-}$ negative, the abscissa for the
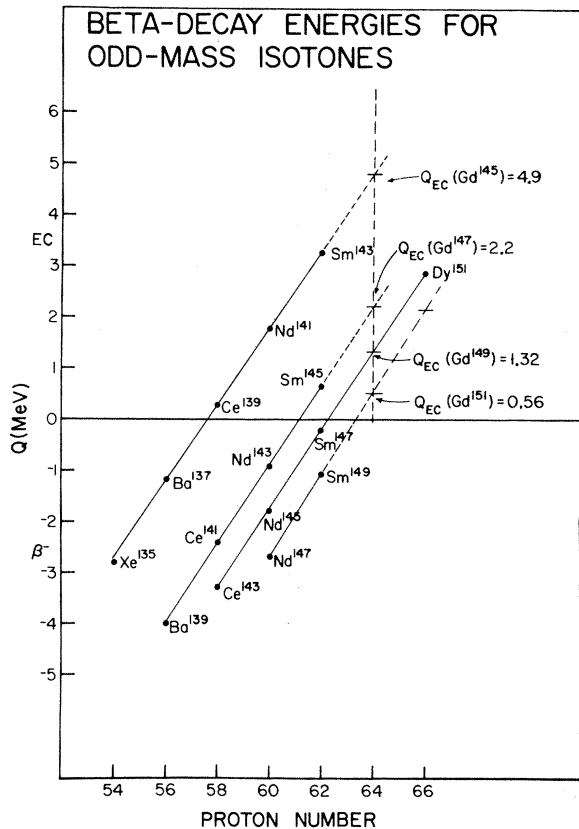former is $Z_{\rm parent}$, and for the latter, $Z_{\rm daughter}$.

FIG. 12. Graphical estimates for the electron-capture decay energies for several odd-mass Gd isotopes, including $Gd^{149}$. For example, the decay energy for $Gd^{149}$ is estimated by plotting all known decay energies versus the proton number (for both $\beta^+/\epsilon$ and $\beta^-$ decay) which involve nuclear pairs having a neutron change of $85 \rightarrow 86$ or $86 \rightarrow 85$. The resulting straight line allows the value of 1.32 MeV to be interpolated for the decay of $Gd^{149}$.

For example, in estimating $Q_\epsilon$ for $Gd^{149}$, the experimental decay energies of all pairs with $N = 85 \rightarrow 86$ or $N = 86 \rightarrow 85$ were plotted. As can be seen from Fig. 12, these points all fall on a straight line, and $Q_\epsilon$ for $Gd^{149}$ can be read from the same line. Using this method we estimate $Q_\epsilon$ as 1.320 MeV. The plots for $Gd^{145}$, $Gd^{147}$, and $Gd^{151}$ have also been included for reference. As read from the graph, $Q_\epsilon$ for these isotopes is 4.9, 2.2, and 0.56 MeV, respectively. These compare with previous estimates of 5,[24] 1.8,[25] and 0.4 MeV.[25]

In essence, this method involves taking the difference between two parabolas cutting across the mass surface and assumes that there are no appreciable bumps or ridges to distort the surface in the region involved. Had we chosen to make a similar plot based on proton pairs rather than neutron pairs, it is easy to see that the $N = 82$ shell would have introduced a serious distortion. Al-

though there is no formal justification for the plot we did make, the fact that no major proton shells or subshells are likely to be encountered means that such estimates for $Q_\epsilon$ should be reasonably reliable.

## V. PROPOSED DECAY SCHEME

On the basis of the foregoing coincidence, delayed-coincidence, and anticoincidence spectra, aided by energy sums and intensity balances, we have placed excited states in $Eu^{149}$ as indicated by our decay scheme, which is presented in Fig. 13. The results of our $\gamma$-ray energy and intensity measurements, conversion coefficients, and assigned transition multipolarities are summarized in Table VI. Unfortunately, as we have intimated earlier, the preparation of clean $Gd^{149}$ sources free from subtle contaminants is not a trivial task, and many incorrect transitions and states have accrued in the literature. Thus, we have included in our decay scheme only those states that were actually indicated by *experiments* in our laboratory. To ameliorate this inflexible position somewhat, we have included in Fig. 13, to the side of our decay scheme, some placements that we could neither confirm not deny and which appear to be reasonable. For the most part these originate from the conversion-electron work of Harmatz and Handley,[11] who observed a number of transitions too weak to be detectable in $\gamma$-ray spectra.

Specific evidence for our placing of each level and its associated transitions follows:

*149.6-keV level.* The 149.6-keV peak is by far the most intense transition in the $\gamma$-ray spectrum. If this were not a ground-state transition, we should see other transitions of comparable intensity that would deexcite the level fed by the strong 149.6-keV transition. Therefore, in agreement with all previous workers, we place the first excited state near 150 keV, specifically, at 149.6 keV. This is also consistent with an overwhelming mass of systematics showing that odd-proton nuclei with $51 \le Z \le 63$ have $\frac{5}{2}^+$ or $\frac{7}{2}^+$ ground states or first excited states separated by an energy rarely greater than 150 keV.

The coincidence experiment having its gate on the 149.6-keV peak (Fig. 5) showed enhanced peaks at 272.0, 346.5, 516.4, 645.2, 663.3, 788.6, and 947.7 keV. These results agree with those of Jaklevic, Funk, and Mihelich,[6] with the exception of the 663.3-keV peak, which they did not see in a coincidence spectrum. All of these transitions can thus be considered as feeding the 149.6-keV level, and it will be shown later that, with the exception of the 272.0-keV $\gamma$, all feed it directly.
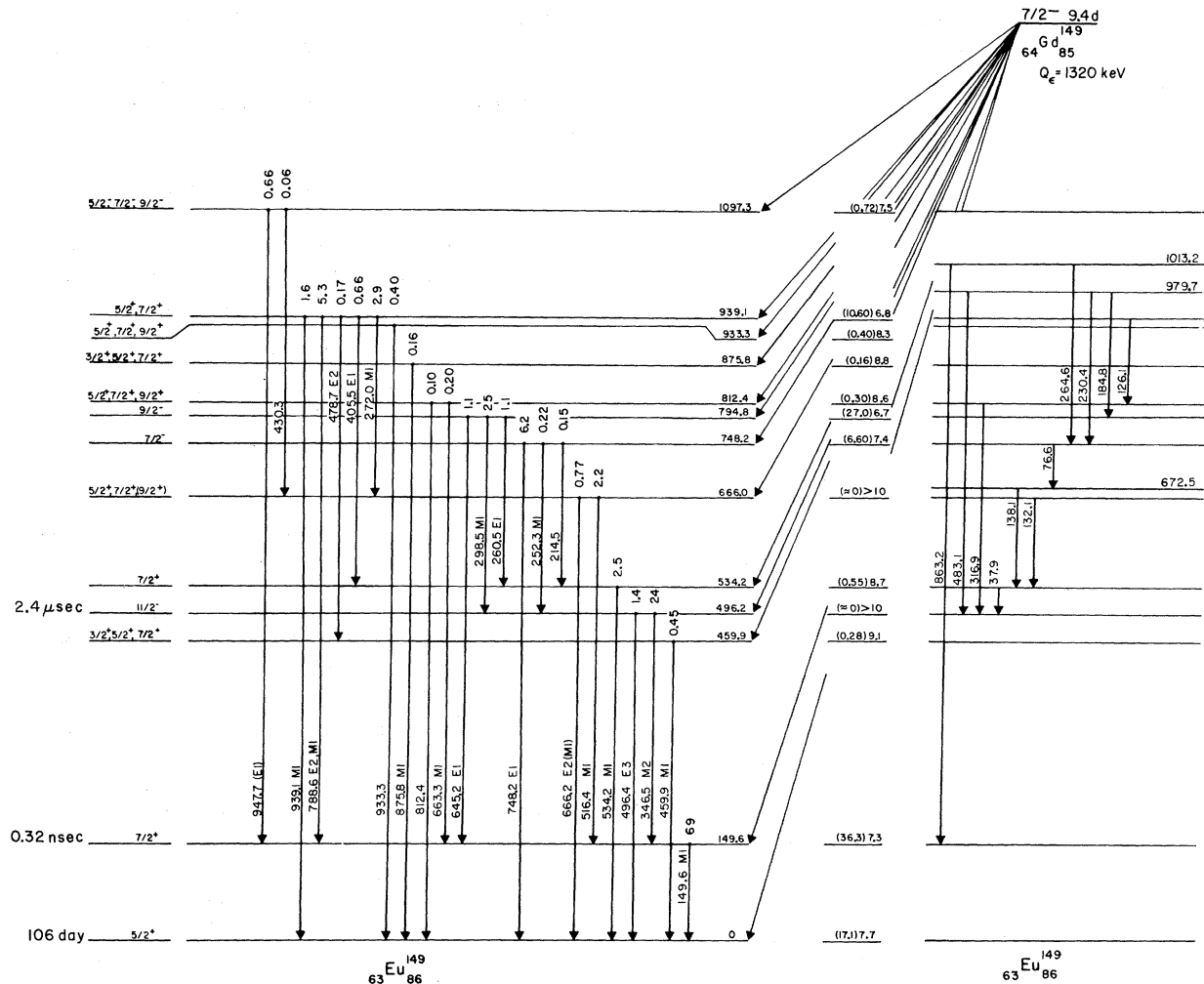
The 149.6-keV coincidence spectrum, in conjunc-

FIG. 13. Decay scheme of Gd[149]. The scheme shown at the left is our proposed decay scheme. All energies are given in keV and (total) transition intensities are given in percent of the disintegrations of Gd[149]. The percent decay to each level (in parenthesis) and the log$ft$ values are listed at the right side of the level scheme. The skeletal scheme shown at the right of the figure shows the same levels as at the left, with the addition of three levels and the addition of electromagnetic transitions for which electrons have been reported but for which no $\gamma$ rays have been observed. These extra levels and transitions are those reported by Harmatz and Handley (Ref. 11). All of their electron transitions that are compatible with our proposed scheme have been included.

tion with the singles spectra, made it possible to determine the energies of the peaks in the 663.3-666.2-keV doublet more precisely than before. As only the 663.3-keV $\gamma$ was in coincidence with the 149.6-keV $\gamma$, its energy and intensity could be determined directly from the coincidence spectrum. These values were then used to subtract the 663.3-keV peak from the singles doublet, leaving the 666.2-keV peak quite well determined by the difference.

*459.9-keV level.* Owing to the results of the delayed coincidence spectra (Fig. 10), the 459.9-keV $\gamma$ can no longer be considered to be feeding the 496.4-keV level, as had been concluded by pre-

vious workers.[5-7] Also, as seen in Fig. 3 and Table III, this $\gamma$ ray is enhanced in the anticoincidence spectrum but is absent from most of the prompt-coincidence spectra. From this evidence, we place the 459.9-keV $\gamma$ as emanating from a level of this same energy.

On the basis of energy sums, the 478.7-keV $\gamma$ could be placed connecting the 459.9-keV level with the well-established 939.1-keV level (see below). Other evidence for this placement comes from the 534-keV gated spectrum (Fig. 7). While the 459.9-keV peak is less intense than in the singles spectra, it is still present—most likely due to some of the 478.7-keV $\gamma$ in the relatively wide

TABLE VI. Transition data for Gd$^{149}$

| Energy | Photon intensity | K-conversion intensity[a-c] | Total intensity[d] | Experimental $\alpha_K$ | Multipole order |
|---|---|---|---|---|---|
| K x rays | 468 ± 100 | ··· | ··· | ··· | ··· |
| 149.6 ± 0.2 | 233 ± 10.0 | 124.9 | 377 | 0.54 | M1 |
| 214.5 ± 0.6 | 0.81 ± 0.1 | ··· | 0.84 | ··· | ··· |
| 252.3 ± 0.7 | 1.1 ± 0.2 | 0.14 | 1.23 | 0.13 | M1 |
| 260.5 ± 0.3 | 5.8 ± 0.4 | 0.15 | 5.92 | $2.6 \times 10^{-2}$ | E1 |
| 272.0 ± 0.2 | 14.6 ± 0.6 | 1.75 | 16.3 | $1.2 \times 10^{-1}$ | M1 |
| 298.5 ± 0.2 | 127 ± 10 | 10.75 | 138 | 8.5 | M1 |
| 346.5 ± 0.3 | ≡100 | 20.0 | 123 | 0.20 | M2 |
| 405.5 ± 0.7 | 3.7 ± 1.5 | 0.033 | 3.7 | $9.0 \times 10^{-3}$ | E1 |
| 430 | 0.33 ± 0.05 | ··· | 0.33 | ··· | ··· |
| 459.9 ± 0.3 | 2.4 ± 0.19 | 0.073 | 2.49 | $3.0 \times 10^{-2}$ | M1 |
| 478.7 ± 0.3 | 1.0 ± 0.1 | 0.011 | 0.96 | $1.2 \times 10^{-2}$ | E2 |
| 496.4 ± 0.3 | 7.2 ± 0.35 | 0.238 | 7.49 | $3.3 \times 10^{-2}$ | E3 |
| 516.4 ± 0.3 | 11.1 ± 1.5 | 0.213 | 11.3 | $1.9 \times 10^{-2}$ | M1 |
| 534.2 ± 0.3 | 13.2 ± 0.55 | 0.256 | 13.5 | $1.9 \times 10^{-2}$ | M1 |
| 645.2 ± 0.3 | 5.9 ± 0.5 | 0.018 | 5.9 | $3.0 \times 10^{-3}$ | E1 |
| 663.3 ± 0.7 | 1.1 ± 0.2 | 0.016 | 1.10 | $1.5 \times 10^{-2}$ | M1 |
| 666.2 ± 0.7 | 3.9 ± 0.6 | 0.026 | 4.0 | $6.6 \times 10^{-3}$ | E2 |
| 748.2 ± 0.3 | 34.6 ± 4.0 | 0.071 | 34.7 | $2.0 \times 10^{-3}$ | E1 |
| 788.6 ± 0.3 | 29.6 ± 3.0 | 0.15 | 29.8 | $5.1 \times 10^{-3}$ | M1+E2 |
| 812.4 ± 0.5 | 0.55 ± 0.1 | ··· | 0.55 | ··· | ··· |
| 863[e] ? | 0.32 ± 0.1 | weak | ··· | ··· | ··· |
| 875.8 ± 0.4 | 0.90 ± 0.1 | 0.0041 | 0.91 | $4.6 \times 10^{-3}$ | M1 |
| 933.3 ± 0. | 2.2 ± 0.5 | ··· | 2.2 | ··· | ··· |
| 939.1 ± 0. | 9.0 ± 1.4 | 0.044 | 9.0 | $4.9 \times 10^{-3}$ | M1 |
| 947.7 ± 0.5 | 3.7 ± 0.6 | 0.0062 | 3.7 | $1.7 \times 10^{-3}$ | (E1) |

[a]Intensities are from Ref. 11.

[b]Intensities are renormalized such that the $\alpha_K$(346.5 keV) ≡ 0.20.

[c]Errors in the relative intensities are reported as being 15% for the most-intense peaks and increasing for the weaker ones.

[d]For the purpose of arriving at total intensity values, theoretical $L$ and $M$ conversion coefficients were used for the indicated multipolarities. Interpolated values are from Hager and Seltzer (Ref. 20).

[e]Not included in decay scheme.

NaI(Tl) gate. The fact that it is present to more than a very small extent implies that it does not feed the 496.4-keV level, which has a half-life of 2.48 μsec. In Fig. 7 the 459.9- and 478.7-keV γ rays have the same intensity relative to each other as they do in the singles spectra, suggesting again that they are related as above.

*496.2-keV level.* This is the relatively well-known $\frac{11}{2}^-$ isomeric state, again a characteristic of odd-$Z$ nuclei in this region. Its half-life has been measured[19] to be 2.48 ± 0.05 μsec. As a result of this half-life, the transitions to and from this level must be studied by means of delayed-coincidence techniques. From the results of such experiments (Sec. III D, Fig. 10, Table V), only the 252.3- and 298.5-keV γ rays are placed as proceeding to the 496.2-keV level. It is depopulated by the 496.4-keV γ to the ground state (cf. Fig. 3) and by the 346.5-keV γ to the 149.6-keV level (Fig. 5 and Sec. III D). The adopted energy, as for all of the excited states to be discussed, is a weighted

average of these γ rays.

*534.2-keV level.* In the 534-keV gated coincidence spectrum (Fig. 7) the 214.5- and 260.5-keV peaks are most obviously enhanced. Other relatively intense peaks are those at 272.0, 405.5, 459.9, and 478.7 keV, all of which are more intense than can be ascribed to chance coincidences. We have already dealt with the 459.9- and 478.7-keV peaks, and the 272.0-keV peak can be explained by the 516.4-keV γ falling within the gate. This leaves the 405.5-keV γ as feeding the 534.2-keV level, although its coincidence intensity is somewhat less than expected. This coincidence spectrum does not rule out its feeding the 748.2-keV level, which in turn feeds the 534.2-keV level. From energy sums and differences, however, it is one of five γ rays that depopulate the 939.1-keV state, and this is the only placement consistent with our proposed decay scheme.

*666.0-keV level.* The three primary peaks included in the gate for the "600-keV region" coin-

cidence spectrum (Fig. 8) lie at 645.2, 663.3, and 666.2 keV. We have already discussed how the 666.2-keV $\gamma$ appears to be a ground-state transition (above, in the section on the 149.6-keV level), implying the existence of a level at this energy. The peaks in Fig. 8 are those at 149.6, 272.0, 430.3, and perhaps 516.4 keV (crossover timing jitter cut down on the intensity of the latter). That these transitions are involved in cascades is corroborated by the integral-coincidence spectrum. The 149.6-keV coincidence spectrum shows the 516.4-keV $\gamma$ feeding the 149.6-keV level; if we try to place it as feeding this level indirectly through some higher level we obtain no consistency whatever with the remainder of the decay scheme and very quickly exceed the available decay energy. Thus, it depopulates the 666.0-keV level.

The 272.0- and 430.3-keV $\gamma$'s feed into the 666.0-keV level from the 933.3- and 1097.3-keV levels, respectively. These placements are the only ones supported by energy sums.

*748.2- and 812.4-keV levels.* The 748.2- and 812.4-keV $\gamma$'s were indicated to be ground-state transitions by the anticoincidence spectrum. In addition, the 534.2-keV coincidence (Fig. 7) and the delayed coincidence (Fig. 10) spectra indicated our placement of the 214.5- and 252.3-keV $\gamma$'s, making the level at 748.2 keV reasonably certain. Similarly, the enhancement of the 663.3-keV $\gamma$ in the 149.6-keV gated spectrum adds confidence to the placement of a level at 812.4 keV, which had not been adduced by previous workers (the 812.4-keV $\gamma$ had been variously assigned).

*794.8-keV level.* There are no transitions to the ground state from this level, probably because of the proposed high spin of the state. However, each of the transitions leading from it was enhanced in the appropriate coincidence spectrum – 260.5 keV in Figs. 4 and 7, 298.5 keV in Fig. 10, and 645.2 keV in Figs. 4 and 5.

*875.8-keV level.* Perhaps the least certain level in our decay scheme, this placement rests solely on the enhancement of the 875.8-keV $\gamma$ in the anticoincidence spectrum and its suppression in all of the coincidence experiments. Also, there is no other position consistent with the remainder of the decay scheme in which to put it.

*933.3-, 939.1-, and 1097.3-keV levels.* In the "900-keV-region" gated coincidence spectrum (Fig. 9), the only peak present is the one at 149.6 keV. From the integral-, 149.6-keV-gated, and anticoincidence spectra, it is evident that the 947.7-keV $\gamma$ is the only one in coincidence. It indicates a level at 1097.3 keV, which is corroborated by the enhancement of the 430.3-keV $\gamma$ to the 666.0-keV level, as discussed above. The 933.3-keV level is placed on the basis of its sole transition to the

ground state. The 939.1-keV level, on the other hand, depopulates by five $\gamma$ rays, all of which are confirmed by coincidence spectra, as discussed above under the sections concerning the levels to which each feeds.

## VI. DISCUSSION

$_{63}Eu^{149}_{86}$, with four neutrons above the $N = 82$ closed shell, must have its structure interpreted cautiously. Although the closed shell is only four neutrons away in one direction, well-defined rotational structure makes its appearance[26] at $Eu^{153}$, only four neutrons in the other direction. This means that when discussing states in $Eu^{149}$ one must be careful not to draw arbitrary conclusions from the spherical shell model and must be prepared to accept collective effects and the fractionation of single-particle strengths over many states.

That $Eu^{149}$ should be very soft toward vibrational deformations is borne out by the fact that $Sm^{148}$, its even-even core, has a $2^+$ one-phonon vibrational state[27] at only 551 keV, a $3^-$ (octupole?) state at 1162 keV, and a $4^+$ (from the two-phonon vibrational triplet?) at 1181 keV.

The simple shell model predicts that above $Z = 50$ the available proton orbits are $g_{7/2}$ and $d_{5/2}$ lying close together, then, after a gap of a few hundred keV, $h_{11/2}$, $s_{1/2}$, and $d_{3/2}$. The parent, $Gd^{149}$, should have eight $g_{7/2}$ and six $d_{5/2}$ protons (or some distribution of proton pairs in these nearly degenerate orbits) outside the $Z = 50$ closed shell. Its last three neutrons should lie in $h_{9/2}$ and/or $f_{7/2}$ orbits, the unpaired neutron being in the $f_{7/2}$ orbit, similar to many other $I^\pi = \frac{7}{2}^-$ nuclei above $N = 82$. (This neutron assignment involves somewhat circular logic connected with the $Gd^{149}$ $\epsilon$-decay properties, but no other assignment gives any sort of consistent picture.)

Similarly, the ground state of $Eu^{149}$ can be characterized as $(g_{7/2})^8(d_{5/2})^5$ protons above $Z = 50$ and $(h_{9/2})^4$ or $(f_{7/2})^4$ (or some combination) neutrons above $N = 82$. This $\frac{5}{2}^+$ configuration is well established from its $\epsilon$ decay[28] and again is consistent with many odd-$Z$ nuclei in this region. The first excited state undoubtedly has a $g_{7/2}$ proton hole as a major component in its configuration, i.e., $(g_{7/2})^7(d_{5/2})^6$, again in agreement with many other odd-$Z$ nuclei in the region. These assignments are consistent with the 0.32-nsec half-life[29] of the 149.6-keV state, a half-life quite in line with $l$-forbidden $M1$ transitions between $g_{7/2}$ and $d_{5/2}$ states.

The $\epsilon$ decay to the ground and 149.6-keV states demonstrates quite clearly that they are separate single-particle states and not members of a $K = \frac{5}{2}$ rotational band. From our above assignments the $\epsilon$ decay can be pictured as $\pi d_{5/2} \to \nu f_{7/2}$ for the

ground state and $\pi g_{7/2} \to \nu f_{7/2}$ for the 149.6-keV state. The observed branchings (and $\log ft$'s), 17.1% (7.7) and 36.3% (7.3), are perfectly consistent with such transitions. On the other hand, if the 149.6-keV state were the $\frac{7}{2}^+$ member of a $K = \frac{5}{2}$ rotational band, the relative $\epsilon$ population should be predictable by the ratio of the squares of the following vector-coupling coefficients:

$$\frac{\langle I_i K_i l (K_f - K_i) | I_i l I_f K_f \rangle^2_{\text{excited}}}{\langle I_i K_i l (K_f - K_i) | I_i l I_f K_f \rangle^2_{\text{ground}}} = \frac{\langle \frac{7}{2} \frac{7}{2} 1 -1 | \frac{7}{2} 1 \frac{7}{2} \frac{5}{2} \rangle^2}{\langle \frac{7}{2} \frac{7}{2} 1 -1 | \frac{7}{2} 1 \frac{5}{2} \frac{5}{2} \rangle^2} = \frac{1}{3} .$$

This is clearly in the wrong direction even before the energy dependence has been included.

The only other simple single-particle state that can be clearly identified is the $h_{11/2}$ state at 496.2 keV. The measured $M2$ and $E3$ multipolarities of the 346.5- and 496.4-keV transitions indicate the $\frac{11}{2}^-$ assignment, as does the $2.48 \pm 0.05$-$\mu$sec half-life of the state. Single-particle estimates[30] for the half-lives of the $M2$ and $E3$ are $3.8 \times 10^{-8}$ and $8.2 \times 10^{-5}$ sec, respectively, to be compared with the measured partial half-lives of $2.7 \times 10^{-6}$ and $3.6 \times 10^{-5}$ sec. The $M2$ is retarded by a factor of approximately 70, but then, $M2$'s are commonly retarded by such factors. More surprising, the $E3$ is enhanced by a factor of about 2.3 over its single-particle estimate, and most $E3$'s are also retarded. However, there are three other known enhanced $E3$ transitions,[31,32] in $La^{137}$, $Pr^{139}$, and and $Eu^{147}$, all nuclei just above or below $N = 82$ and all involving an $h_{11/2}$ state. A cursory attempt[32] has been made to explain the enhancements on the basis of octupole-coupled admixtures of the ground states in the $h_{11/2}$ states, but at this point meaningful quantitative calculations cannot be made. However, the assignment of the 496.2-keV state as an $h_{11/2}$ state is warranted, and its receiving no direct $\epsilon$ population from $Gd^{149}$ is consistent with this assignment.

A number of spin and parity assignments can be made for the other states, but deciding much about their internal structures is quite difficult. Many of the states are undoubtedly core coupled, e.g., the 459.9- and 534.2-keV states, but most conclusions at this point would be somewhat arbitrary. Unfortunately, theoretical studies of this region are all but nonexistant, and even useful experimental systematics are scarce. We are currently studying other nearby Gd isotopes and hope to be able to say more about the structures of states in the various nuclei in this region at the conclusion of these studies. Meanwhile, in this paper we confine ourselves to a more or less straightforward discussion of the spins and parities *per se*, as they can be deduced from the $\gamma$ transitions. The $\epsilon$ decay

itself yields little information, for most of the $\log ft$ values lie in the range which indicates either first-forbidden or allowed transitions, and it will be necessary to know more about the internal structures of the states before drawing serious conclusions from these values.

The 459.9-keV state can be assigned $\frac{3}{2}^+$, $\frac{5}{2}^+$, or $\frac{7}{2}^+$ because of the $M1$ character of its ground-state $\gamma$-ray transition. The $\log ft$ value of 9.1 seems to imply a first-forbidden unique transition. However, if one considers this state as arising from core coupling to the one-phonon 551-keV state in $Sm^{148}$, the $\log ft$ value would be expected to be larger than normal. With this in mind, the $\epsilon$ decay could in fact be a normal first-forbidden transition. Consequently, the spin assignment for the 459.9-keV state cannot be narrowed down from the above. And if the $d_{5/2}$ ground state were the single-particle component of the core-coupled state, this could easily explain the absence of a transition to the 149.6-keV state.

The 534.2-keV state can also be assigned $\frac{3}{2}^+$, $\frac{5}{2}^+$, or $\frac{7}{2}^+$ because of the $M1$ character of its ground-state transition. It is also tempting to think of this state as the $d_{5/2}$ ground state coupled to the $2^+$ quadrupole vibrational state. We shall see below that the assignment for the 534.2-keV state can be narrowed down to $\frac{7}{2}^+$.

The 666.0-keV state is limited to $\frac{5}{2}^+$, $\frac{7}{2}^+$, or $\frac{9}{2}^+$ by the $M1$ transition to the 149.6-keV state. If, as it appears, the 666.2-keV transition to the ground state does have appreciable $M1$ admixing in its $E2$ character, the $\frac{9}{2}^+$ possibility is eliminated.

Assignments for the next two states, at 748.2 and 794.8 keV, can be much more specific because of the many $\gamma$-ray branches proceeding from them. The 748.2-keV $E1$ $\gamma$ implies a spin of $\frac{3}{2}^-$, $\frac{5}{2}^-$, or $\frac{7}{2}^-$ for the 748.2-keV state. The 252.3-keV $\gamma$ to the $\frac{11}{2}^-$ state appears to be an $M1$, which is inconsistent with the 748.2-keV $\gamma$ being an $E1$. However, assuming the 252.3-keV $\gamma$ to be really an $E2$ narrows the choice for the 748.2-keV state to $\frac{7}{2}^-$. The $\log ft$ of 7.4 is somewhat high for an allowed transition, but remembering that the 748.2-keV state undoubtedly has a complex structure, one would expect a $\beta$ transition to it to be hindered. With a $\frac{7}{2}^-$ assignment, the 214.5-keV $\gamma$ to the 534.2-keV state allows the narrowing of assignments for the latter down to $\frac{5}{2}^+$ or $\frac{7}{2}^+$.

The strong 298.5-keV $M1$ transition from the 794.8-keV state to the 496.4-keV state suggests the possibilities $\frac{9}{2}^-$, $\frac{11}{2}^-$, or $\frac{13}{2}^-$ for the upper state. The 645.2-keV $E1$ transition to the 149.6-keV state limits the choice to $\frac{9}{2}^-$. The $\log ft$ for $\epsilon$ decay to this state is the lowest for decay to any state, implying that this transition, if any, is allowed, again consistent only with the $\frac{9}{2}^-$ assignment. The 260.5-

keV $E1$ $\gamma$ then allows the assignment for the 534.2-keV state to be narrowed further to $\frac{7}{2}^+$.

If we may be forgiven a little speculation at this point, a word about one component of the wave function of the 794.8-keV state might perhaps be in order. Consider the two facts: (1) A relatively simple mechanism must exist for populating the state so readily from $Gd^{149}$, and (2) the abnormally large intensity of the transition to the 496.4-keV state indicates a similarity to that state. Now, there is ample indication[33-35] that, below $N = 82$ at least, there is appreciable $h_{11/2}$ character in the proton pairs of the Gd isotopes, and this should also be true here. Any $\epsilon$ transitions from $Gd^{149}$ involving $g_{7/2}$ or $d_{5/2}$ protons would not be expected to proceed at all rapidly to the available final neutron states, nor would they lead to $\frac{9}{2}^-$ over-all final states. On the other hand, a $\pi h_{11/2} \to \nu h_{9/2}$ transition not only would proceed relatively quickly, but also it would lead to the final configuration, $(\pi h_{11/2})(\nu h_{9/2})(\nu f_{7/2})$, which could furnish a $\frac{9}{2}^-$ state among its couplings. Similar cases, resulting in three-particle final states are known[31,36] in the $N = 82$ region, although the three-particle states lie considerably higher than 794.8 keV. Thus, although we do not suggest this as the primary component of the 794.8-keV state, such an admixture would account satisfactorily for the $\epsilon$ decay.

The state at 812.4 keV is assigned $\frac{5}{2}^+$, $\frac{7}{2}^+$, or $\frac{9}{2}^+$ on the basis of its ground-state $\gamma$ transition and the 663.3-keV $M1$ transition to the 149.6-keV state. A possible $\frac{3}{2}^+$ assignment for this state is ruled out on the argument that the large $\log ft$ is probably a result of internal complexities in the state necessitating multiparticle rearrangement during the $\epsilon$ decay rather than the $\epsilon$ decay being first-forbidden unique.

The single $\gamma$ transition of 875.8 keV emanating

from the state of this energy is assigned an $M1$ multipolarity. This limits the state spin to $\frac{3}{2}^+$, $\frac{5}{2}^+$, or $\frac{7}{2}^+$, assignments that are compatible with the $\epsilon$ decay to this state.

Harmatz and Handley[11] do not report conversion-electron intensity values for the 933.3-keV transition. Therefore, we cannot make a definite spin assignment to the 933.3-keV state on the basis of this transition. From the $\log ft$ value of 8.3, assuming this again to be a hindered first-forbidden transition, the spin could be $\frac{5}{2}^+$, $\frac{7}{2}^+$, or $\frac{9}{2}^+$.

The 939.1-keV $M1$ ground-state transition suggests $\frac{3}{2}^+$, $\frac{5}{2}^+$, or $\frac{7}{2}^+$ for the 939.1-keV state. The 788.6-keV transition (if it really contains an appreciable $M1$ admixture) eliminates the $\frac{3}{2}^+$ possibility, as does the relatively low $\log ft$ value of 6.8. Neither the 478.7- nor the 272.0-keV $\gamma$'s allow this to be narrowed further. It should be noted that an $E1$ multipolarity for the 405.5-keV transition, while experimentally indicated, is incompatible with the other assignments. A three-particle final-state component can also be invoked here to explain the $\epsilon$ decay, this time a $\pi g_{7/2} \to \nu h_{9/2}$ transition resulting in $(\pi g_{7/2})^{-1}(\nu h_{9/2})(\nu f_{7/2})$ as a component of the final state.

The 947.7-keV $E1$ transition implies $\frac{5}{2}^-$, $\frac{7}{2}^-$, or $\frac{9}{2}^-$ for the 1097.3-keV state. The $\log ft$ is compatible with any of these possibilities, but other than this, little can be deduced about the state.

## ACKNOWLEDGMENTS

---

[1] P. Alexander, Phys. Rev. 134, B499 (1964); T. Cretzu, K. Holmuth, and G. Winter, Nucl. Phys. 56, 415 (1964).

[2] V. S. Shirley and J. O. Rasmussen, Phys. Rev. 109, 2092 (1958); E. Steichele and P. Kienle, Z. Physik 175, 405 (1963).

[3] R. W. Hoff, J. O. Rasmussen, and S. G. Thompson, Phys. Rev. 83, 1068 (1951).

[4] V. S. Shirley, W. G. Smith, and J. O. Rasmussen, Nucl. Phys. 4, 395 (1957).

[5] H. J. Prask, J. J. Reidy, E. G. Funk, and J. W. Mihelich, Nucl. Phys. 36, 441 (1962).

[6] J. M. Jaklevic, E. G. Funk, and J. W. Mihelich, Nucl. Phys. 84, 618 (1966).

[7] I. Adam, K. S. Toth, and R. A. Meyer, Nucl. Phys. A106, 275 (1968).

[8] N. M. Anton'eva, A. A. Bashilov, B. S. Dzhelepov, and B. K. Preobrazhenskii, Izv. Akad. Nauk SSSR Ser. Fiz. 22, 895 (1958) [transl.: Bull. Acad. Sci. USSR, Phys. Ser. 22, 889 (1958)].

[9] V. K. Adamchuk, A. A. Bashilov, and B. K. Preobrazhenskii, Izv. Akad. Nauk SSSR Ser. Fiz. 22, 919 (1958) [transl.: Bull. Acad. Sci. USSR, Phys. Ser. 22, 911 (1958)].

[10] B. S. Dzhelepov, B. K. Preobrazhenskii, and V. A. Sergienko, Izv. Akad. Nauk SSSR, Ser. Fiz. 23, 219 (1959) [transl.: Bull. Acad. Sci. USSR, Phys. Ser. 23, 211 (1959)].

[11] B. Harmatz and T. H. Handley, Nucl. Phys. 81, 481 (1966).

[12] A. Siivola and G. Graeffe, Nucl. Phys. 64, 161 (1965).

[13]R. N. Keller, reported in P. C. Stephenson and W. E. Nervik, Radiochemistry of the Rare Earths, Scandium, Yttrium, and Actinium, "Nuclear Science Series," Nuclear Research Council, Committee on Nuclear Science, Report No. NAS-NS 3020, 1961 (unpublished).

[14]G. R. Choppin, B. G. Harvey, and S. G. Thompson, J. Inorg. Nucl. Chem. 2, 66 (1956).

[15]S. G. Thompson, B. G. Harvey, G. R. Choppin, and G. T. Seaborg, J. Am. Chem. Soc. 76, 6229 (1954).

[16]MOIRAE, an oscilloscope code developed primarily by R. Au and G. Berzins for use on the Michigan State University Sigma 7 computer in the Cyclotron Laboratory.

[17]L. Nemet, Izv. Akad. Nauk SSSR Ser. Fiz. 25, 68 (1961) [transl.: Bull. Acad. Sci. USSR, Phys. Ser. 25, 68 (1961)].

[18]R. L. Auble, D. B. Beery, G. Berzins, L. M. Beyer, R. C. Etherton, W. H. Kelly, and Wm. C. McHarris, Nucl. Instr. Methods 51, 61 (1967).

[19]E. E. Berlovich, V. N. Klementyev, L. V. Krasnov, M. K. Nikitin, and I. Yursik, Nucl. Phys. 23, 481 (1961).

[20]R. S. Hager and E. C. Seltzer, Nucl. Data 4A, 1 (1968).

[21]M. P. Avotina, as quoted in Ref. 7.

[22]Reference 11, using the results of P. A. Seeger, Nucl. Phys. 25, 1 (1961).

[23]K. Way and M. Wood, Phys. Rev. 94, 119 (1954).

[24]J. R. Grover, Phys. Rev. 116, 406 (1959).

[25]J. H. E. Matlauch, W. Thiele, and A. H. Wapstra,

Nucl. Phys. 67, 1, 32, 73 (1965).

[26]P. Alexander, F. Boehm, and E. Kankeleit, Phys. Rev. 133, B284 (1964).

[27]C. V. K. Baba, G. T. Ewan, and J. F. Suárez, Nucl. Phys. 43, 264, 285 (1963).

[28]B. Harmatz, T. H. Handley, and J. W. Mihelich, Phys. Rev. 123, 1758 (1961).

[29]E. E. Berlovich, Yu. K. Gusev, V. V. Ilin, V. V. Nikitin, and M. K. Nikitin, Zh. Eksperim. i Teor. Fiz. 42, 967 (1962) [transl.: Soviet Phys.—JETP 15, 667 (1962)].

[30]S. A. Moszkowski, in *Alpha-, Beta-, and Gamma-Ray Spectroscopy*, edited by K. Siegbahn (North-Holland Publishing Company, Amsterdam, The Netherlands, 1965); S. A. Moszkowski, Phys. Rev. 89, 474 (1953).

[31]D. B. Beery, W. H. Kelly, and Wm. C. McHarris, Phys. Rev. 188, 1851 (1969).

[32]J. R. Van Hise, G. Chilosi, and N. J. Stone, Phys. Rev. 161, 1254 (1967).

[33]R. E. Eppley, Wm. C. McHarris, and W. H. Kelly, to be published; also in Michigan State University Report No. COO-1779-13, 1969 (unpublished), p. 55.

[34]J. Felsteiner and B. Rosner, Phys. Letters 31B, 12 (1970).

[35]B. H. Wildenthal, Michigan State University, private communication.

[36]Wm. C. McHarris, D. B. Beery, and W. H. Kelly, Phys. Rev. Letters 22, 1191 (1969).

# $g$ Factors of the First Two Excited $2^+$ States in Pt$^{192}$†

Z. W. Grabowski

*Department of Physics, Purdue University, Lafayette, Indiana 47907*

(Received 16 February 1970)

The $g$ factors of the first and the second excited $2^+$ state in Pt$^{192}$ have been measured by observing the integral rotation of the directional correlation pattern in the internal magnetic field acting on Pt nuclei implanted in an iron host. Both values, $g_{316} = 0.27 \pm 0.02$ and $g_{612} = 0.30^{+0.06}_{-0.04}$, are higher than those predicted by the pairing-plus-quadrupole model of Kumar and Baranger.

## I. INTRODUCTION

Magnetic moments of excited nuclear states of even W, Os, and Pt nuclei were predicted by Kumar and Baranger on the basis of the pairing-plus-quadrupole model.[1] For spherical nuclei in this region the predicted values of the $g$ factors are considerably more reduced with respect to $Z/A$ (hydrodynamic value) than $g$ factors derived from the model proposed by Greiner.[2] Measurements of the mixing ratios of the $\gamma$ transitions[3] in Pt$^{192}$ show surprisingly good agreement with pairing-plus-quadrupole model calculations of Kumar.[4] It was of interest, therefore, to check the agreement between experiment and theory also for the $g$ factors of the first two excited $2^+$ states in the

same nucleus. The "physical boson mixing theory" proposed by Ikegami and Hirata,[5] which was able to explain small measured values of the pentration parameter ($\lambda \approx 1$) for the strongly hindered $M1$ component between the first and second excited $2^+$ states in spherical nuclei of the Pt region,[6] predicted $|g_{2^+_1}| > |g_{2^+_2}|$ for those nuclei.

## II. EXPERIMENTAL PROCEDURE AND RESULTS

The levels in Pt$^{192}$ were populated from the decay of Ir$^{192}$ (Fig. 1). The $g$ factors of the first two excited $2^+$ states in Pt$^{192}$ were measured using the time-integrated directional-correlation method.[8] In view of the short lifetimes of the states, the internal field acting on Pt nuclei embedded in an